PHYSICAL REVIEW B, VOLUME 64, 060104(R)

Systematics of group-nonsubgroup transitions: Square to triangle transition

D. M. Hatch,[1,2] T. Lookman,[1] A. Saxena,[1] and H. T. Stokes[2]
[1]*Theoretical Division, Los Alamos National Laboratory, Los Alamos, New Mexico 87545*
[2]*Department of Physics and Astronomy, Brigham Young University, Provo, Utah 84602*
(Received 26 January 2001; revised manuscript received 20 February 2001; published 19 July 2001)

A variety of structural transitions in nature do not involve a group-subgroup relationship. A two-dimensional example is the transition between a square lattice and a triangular lattice, which is known to occur in vortex lattices, Wigner crystals, skyrmion lattices, colloids, diblock copolymers, etc. A three-dimensional analog is the shock-induced BCC to HCP transition in iron. We develop a systematic technique that incorporates site symmetry and yields displacive transition mechanisms and free energy forms for such structural changes. This procedure is demonstrated for the square to triangle transition.

DOI: 10.1103/PhysRevB.64.060104 PACS number(s): 81.30.Kf, 64.70.Kb, 05.70.Fh

Landau theory of phase transitions is readily applicable to those transitions in which the parent and product phases have a group-subgroup relationship. However, examples of transitions abound in nature where no group-subgroup relation exists in the two ordered phases of different symmetry.[1] A prime example is the martensitic transition from a body-centered cubic (bcc) to a hexagonal close-packed (hcp) phase in iron that occurs at $\sim$13 GPa. A two-dimensional (2D) analog is the square lattice to triangular lattice transformation which is observed in a wide variety of disparate physical systems.

In these transitions various mechanisms involve different distortion paths in which site symmetries play a crucial role. Therefore one must go beyond the conventional Landau theory and include this information in the description of the structural change.

To accomplish this, we use the reconstructive square to triangle transition as an example and (i) extend the Landau theory to incorporate local site symmetric information, (ii) propose a symmetry based algorithm that allows us to enumerate paths, (iii) identify the primary and secondary order parameters (OP's) for each path and establish the corresponding Ginzburg-Landau free energy, and (iv) for a specific path, embed the special end point of the primary OP as a function of local distortions.

We believe this systematic algorithmic procedure is quite general and provides practical implementation of a broad study of transition mechanisms and the resulting free energies. In our procedure we obtain displacive transition mechanisms grouped according to irreducible representations (IR's) and provide primary and secondary OP displacement paths. The OP's for each mechanism provide a single thermodynamic free energy representing the end phase as well as the intermediary phase. We have consistently applied our procedure to several three-dimensional (3D) transitions and checked the implications against electronic structure calculations.

Site-specific Landau theory. The conventional Landau theory of phase transitions assumes the change in density is written in terms of basis functions of the IR of the original parent space group G. For example

$$\delta\rho(\mathbf{r}) = \sum_{\mathbf{k}_\alpha,\gamma,i} \eta_i^{\mathbf{k}_\alpha,\gamma} \psi_i^{\mathbf{k}_\alpha,\gamma}(\mathbf{r}) \tag{1}$$

is a symmetry expansion of the density function where the wave vector $\mathbf{k}$ is in the first Brillouin zone, α labels the IR, γ references different copies of the IR, and i labels the basis functions of the IR. The coefficients in this expansion, $\eta_i^{\mathbf{k}_\alpha,\gamma}$, can be interpreted as carrying the transformation properties. The formalism describes small changes from the parent structure and the essential features of this change can be carried by these spatially independent ''global'' coefficients. This lack of reference to the *intracell* details makes the Landau theory quite general and easy to implement.

In many structural changes the ''atomic'' displacements are large and, for special values of the displacements, lead to an increase in the symmetry of the structure. The relationship between the beginning and end symmetry is *not* group-subgroup. When considering structural changes for such transitions it is necessary to incorporate specific reference to the local displacements of the atoms and delineate the special value(s) which determines the final structure. This connection has been formulated by using a method of induced representations.[2] The local displacements of an atom relative to the unit cell at the site $\mathbf{r}_0$ can be grouped as the basis functions $\psi_i^H(\mathbf{r})$ of IR's Γ^H. The IR Γ^H is an IR of the point group H of the site $\mathbf{r}_0$. A global representation of the entire space group G is then obtained as

$$\psi_i^{\mathbf{k}_\alpha,\gamma}(\mathbf{r}) = \sum_{g\in G} D_{i,j}^{*\mathbf{k}_\alpha,\gamma}(g)\,\theta(g)\,\psi_1^H(\mathbf{r}). \tag{2}$$

Equation (2) is the required extension of the conventional Landau theory which directly incorporates the site symmetry information. Thus, for example, a displacement of an atom relative to the unit cell in the x direction at $\mathbf{r}_0$ will be correlated with the displacement of every other atom in the same crystallographic *orbit* of the Wyckoff position $\mathbf{r}_0$. The correlated displacements of these atoms transform according to the global basis function $\psi_i^{\mathbf{k}_\alpha,\gamma}(\mathbf{r})$ constructed from this local displacement.

Using this *local to global (displacement) construction* an algorithm can be used to obtain possible mechanisms for transitions where the group-subgroup relationship is *not* obeyed. The method is systematic and can be used for any such symmetry relationship. As a prototype of such a procedure we study the tetragonal ($P4mm$) to hexagonal

TABLE I. Common subgroups of *P*4*mm* and *P*6*mm* with matching Wyckoff positions.

Subgroup	IR,OP dir of *P*4*mm*	New Wyckoff	IR,OP dir of *P*6*mm*	New Wyckoff
*Cmm*2(35)	Γ_3,*P*1	2(a) $z'=z$	Γ_5,*P*1	2(a) $z'=z$
Cm(8)	Γ_5,*P*3	2(a) $x'=0$, $z'=z$	Γ_6,*P*2	2(a) $x'=0$, $z'=z$
Cm(8)	Γ_5,*P*3	2(a) $x'=0$, $z'=z$	Γ_6,*P*1	2(a) $x'=0$, $z'=z$
*P*1(1)	Γ_5	1(a) $x'=0$, $y'=0$, $z'=z$	Γ_6	1(a) $x'=0$, $y'=0$, $z'=z$
*Pma*2(28)	M_5,*P*1	2(c) $y'=1/4$, $z'=z$	M_3,*P*1	2(c) $y'=3/4$, $z'=z$
*Pma*2(28)	M_5,*P*1	2(c) $y'=1/4$, $z'=z$	M_4,*P*1	2(c) $y'=1/4$, $z'=z$
*Pma*2(28)	X_4,*P*3	2(c) $y'=0$, $z'=z$	M_3,*P*1	2(c) $y'=3/4$, $z'=z$
*Pma*2(28)	X_4,*P*3	2(c) $y'=0$, $z'=z$	M_4,*P*1	2(c) $y'=1/4$, $z'=z$
*Ima*2(46)	A_5,*P*1	4(b) $y'=1/4$, $z'=1/2+1/2z$	L_3,*P*1	4(b) $y'=1/4$, $z'=1/2+1/2z$
*Ima*2(46)	A_5,*P*1	4(b) $y'=1/4$, $z'=1/2+1/2z$	L_4,*P*1	4(b) $y'=1/4$, $z'=1/2+1/2z$
$Cmc2_1$(36)	Z_5,*P*1	4(a) $y'=0$, $z'=1/2z$	A_6,*P*1	4(a) $y'=0$, $z'=1/2z$
$Cmc2_1$(36)	Z_5,*P*1	4(a) $y'=0$, $z'=1/2z$	A_6,*P*2	4(a) $y'=0$, $z'=1/2z$
$P2_1$(4)	Z_5,*C*1	4(a) $x'=0$, $y'=1/2z$, $z'=z$	A_6,*C*1	4(a) $x'=0$, $y'=1/2z$, $z'=z$

(*P*6*mm*) transition where we restrict displacements to be in the plane perpendicular to the tetragonal axis. The transition mechanisms then effectively describe the square to triangle lattice transitions in 2D. We assume that the transition is diffusionless and takes place by a continuous displacement of the atoms from the *P*4*mm* phase. As a result there is an *intermediary structure* G_s which is a subgroup of *P*4*mm* and at special values of the displacements the supergroup *P*6*mm* is subsequently obtained. Necessarily the intermediary group is a subgroup of *both P*4*mm* and *P*6*mm*. The specific modes of the displacements which drive the structure from *P*4*mm* into the intermediary group G_s and then to the group *P*6*mm* can be obtained through the *induced representation* constructed above.

Enumeration of paths and free energies. In the transition from *P*4*mm* to *P*6*mm* we give a four step algorithm for obtaining the possible paths of structural change. A software program, ISOTROPY, has been developed[3] which allows one to determine a great deal of the information about 3D space groups and their properties and we use it in the steps of the algorithm. The steps are performed in 3D and through projection describe the square to triangle lattice transition. This allows us to demonstrate explicitly the full and direct use of ISOTROPY and indicates its quite general use for a wide range of 3D reconstructive phase transitions, e.g., bcc to hcp or graphite to diamond transitions.

(1) *Subgroups common to both groups.* For the space group *P*6*mm* Stokes and Hatch[3] list 95 subgroups of *P*6*mm*. They list only those subgroups obtained through IR's corresponding to points of symmetry in the Brillouin zone and corresponding to one primary OP. We will consider only such IR's in our procedure since these are the most likely candidates for initial consideration. Of that list 46 are also subgroups of *P*4*mm*. Since the intermediary group is to be a subgroup of both, only these 46 are viable candidates.

(2) *Subgroups which then have compatible Wyckoff positions.* In connecting the two phases atoms cannot be created nor destroyed. In the *P*4*mm* structure there is one kind of atom and these atoms occupy only the Wyckoff 1(a) position. The atoms of P6*mm* also occupy only the 1(a) position in the hexagonal space group. Each of the 46 subgroups obtained in step (1) are obtained by a specific IR from *P*4*mm* and by a specific IR from *P*6*mm*. We must define an atom to atom correspondence throughout the transition. In Table I, column 1, are listed those common subgroups that have consistent Wyckoff occupation numbers. Notice that the number of pos-

TABLE II. Possible mechanisms for the *P*4*mm* to *P*6*mm* transition.

Subgroup	IR of *P*4*mm*	Dir.	G_s basis	G_s origin	Atoms	Displacement	IR of *P*6*mm*
*Cmm*2(35)	Γ_3	*P*1	(1,1,0) (-1,1,0) (0,0,1)	(0,0,0)		ϵ_{xy}	Γ_5
Cm(8)	Γ_5	*P*3	(1,1,0) (-1,1,0) (0,0,1)	(0,0,0)	(0,0,*z*)	[1,1,0]	Γ_6
*P*1(1)	Γ_5	*C*1	(1,0,0) (0,1,0) (0,0,1)	(0,0,0)	(0,0,*z*)	[1,0,0], [0,1,0]	Γ_5
*Pma*2(28)	M_5	*P*1	(1,1,0) (-1,1,0) (0,0,1)	(0,1/2,0)	(0,0,*z*)	[1,-1,0]	M_3
					(0,1,*z*)	[-1,1,0]	
*Pma*2(28)	M_5	*P*1	(1,1,0) (-1,1,0) (0,0,1)	(0,1/2,0)	(0,0,*z*)	[1,-1,0]	M_4
					(0,1,*z*)	[-1,1,0]	
*Pma*2(28)	X_4	*P*3	(2,0,0) (0,1,0) (0,0,1)	(1/2,0,0)	(0,0,*z*)	[0,-1,0]	M_3
					(1,0,*z*)	[0,1,0]	
*Pma*2(28)	X_4	*P*3	(2,0,0) (0,1,0) (0,0,1)	(1/2,0,0)	(0,0,*z*)	[0,-1,0]	M_4
					(1,0,*z*)	[0,1,0]	

sible intermediary subgroups has been reduced to 7 corresponding to 13 possible path connections. We have retained all 3D intermediary subgroups, including those not allowed as IR's in the strict 2D problem, e.g., the Z_5 IR of $P4mmm$ through the subgroup $P2_1$. These will be discarded as we look for appropriate microscopic 2D displacements in the next step of the algorithm.

(3) *Subgroups that are obtained by microscopic displacements or macroscopic strain.* We are considering structural changes which are to take place by the microscopic displacements of the atoms or by macroscopic strain. Using the induced representation procedure mentioned above we now determine which IR's correspond to x,y displacements relative to the unit cell at the Wyckoff 1(a) site of $P4mm$ and also the Wyckoff 1(a) site of $P6mm$. This process reduces the number of intermediary paths to 4. We add a fifth mechanism which is the shear strain Γ_3, of the form ϵ_{xy}. This IR satisfied steps (1) and (2). We include this strain since it is a mechanism corresponding to a shape change of the unit cell even though it does not arise by displacements of the atoms *relative to* the unit cell.

In Table II are listed the subgroups which provide mechanisms for the $P4mm$ to $P6mm$ transition. Since our interest here is in the square to triangle lattice transition, we have kept *only* strain distortions in the plane perpendicular to the tetragonal axis and displacements within this plane. We list information about the common subgroup following Ref. 3 and specifically give the displacement pattern which changes the structure from $P4mm$ to the subgroup structure. We discard the two mechanisms corresponding to the Γ_5 IR. This IR survived step three of our algorithm and corresponds to a pure translational mode and/or to xz and yz strains. But each of these possible mechanisms are not allowed in this 2D consideration.

(4) *Displacive mechanisms for transition paths.* In Table II, column 6, the atomic coordinates of a selection of Wyckoff positons are given which are sufficient to yield the correlated displacement mechanism for the transition through the given subgroup. The displacement vector is shown in column 7. The displacements for other positions in the structure can be obtained by using the basis vectors of the lattice for the repeat distances. In Fig. 1 are shown the three mechanisms for displacements relative to the unit cell, each of which will drive a transition from $P4mm$ toward $P6mm$. The $P6mm$ structure will result only for special values of atomic displacements. For each mechanism we have indicated the primary displacement parameter. For each primary OP there are secondary OP's which necessarily play a roll in the transition mechanism. In Table III we list for each mechanism the primary and secondary OP's, indicate the free energy (to *sixth degree* in the primary OP) and the end-point (lock-in) value of OP's. The algorhithm is finished.

Tolèdano and Dmitriev[1] initially consider three mechanisms for the square to triangle transition. They drop the ϵ_{xy} shear strain mechanism because it has a maximal limit value. This mechanism corresponds to the Γ_3 mechanism in our labeling. The second mechanism they consider arises from parallel shifts of atomic rows. It is equivalent to the previous mechanism so they again do not consider it. The final mechanism they consider is antiparallel displacements of rows of atoms. This particular transition path corresponds to our X_4 mechanism. Thus the transition mechanisms considered by Tolèdano and Dmitriev are contained within our procedure while we obtain *additional* independent paths to those they found. Of particular note are the two independent paths, M_3,M_4 locking into the $P6mm$ structure for each of the M_5 and X_4 IR's of $P4mmm$.

In Tolèdano and Dmitriev[1] it was shown that the supergroup locks in at special values of the atomic shifts. They indicate that these lock-in values and the morphology of the phase diagram are governed by the nonlinear dependence of the OP $\eta^{\mathbf{k}_\alpha,\gamma}(\xi_1,\xi_2,\ldots)$ on the atomic shifts $\xi_1,\xi_2,\ldots$. For the local position dependent OP the Landau minimization becomes

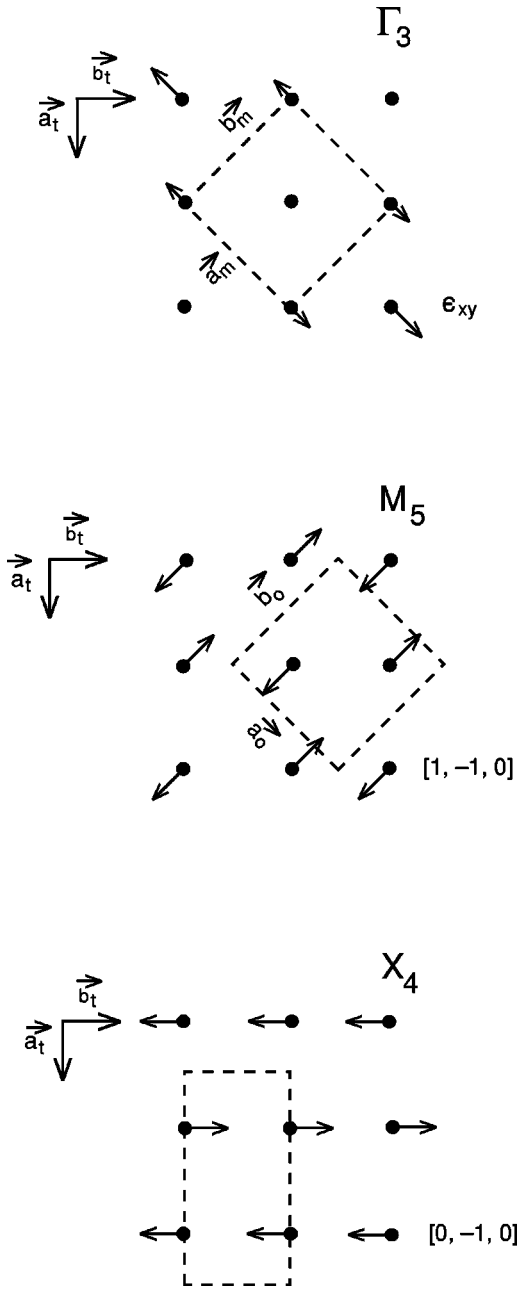

FIG. 1. Deformation paths from the square→ triangular lattice.

TABLE III. Primary and secondary OP's for the $P4mm$ transition and lock-in values corresponding to the $P6mm$ structure. The change in orthorhombic lattice constants ($\vec{a}_o$ and $\vec{b}_o$) in going from the $P4mm$ to the $P6mm$ side of the transition are given in column 5 ($e_1 = \epsilon_{11}+\epsilon_{22}$, $e_2=\epsilon_{11}-\epsilon_{22}$, $e_3=\epsilon_{12}$).

Subgroup	POP	SOP	GL free energy	Lock-in value
$Cmm2(35)$	$\Gamma_3, P1=(e_3)$	$\Gamma_1, P1=(e_1)$	$F_{GL}(35;\Gamma_3)$	$\Gamma_3(\vec{a}_o:\sqrt{2}a\rightarrow\sqrt{3}a;\vec{b}_o:\sqrt{2}a\rightarrow a)$
$Pma2(28)$	$M_5, P1=(\eta_2,0)$	$\Gamma_3, P1=(e_3);\Gamma_1, P1=(e_1)$	$F_{GL}(28;M_5)$	M_5 (small); $\Gamma_3(\vec{a}_o:\sqrt{2}a\rightarrow\sqrt{3}a;\vec{b}_o:\sqrt{2}a\rightarrow a)$
$Pma2(28)$	$X_4, P3=(\eta_3,\eta_3)$	$\Gamma_2, P1=(e_2);\Gamma_1, P1=(e_1)$	$F_{GL}(28;X_4)$	$X_4(a/4);\Gamma_2(\vec{a}_o:2a\rightarrow\sqrt{3}a;\vec{b}_o:a\rightarrow a)$

($\eta_1=e_3, \eta_2=\mathrm{M}_5$ atomic shuffle, $\eta_3=\mathrm{X}_4$ atomic shuffle, $\eta_4=e_1, \eta_5=e_2$)

$F_{GL}(35;\Gamma_3)=A_1^{(1)}\eta_1^2+A_2^{(1)}\eta_1^4+A_3^{(1)}\eta_1^6+g_1^{(1)}(\eta_{1,x}^2+\eta_{1,y}^2)+F_C(\Gamma_3,\Gamma_1)+F_L(\Gamma_1)$

$F_{GL}(28;M_5)=A_1^{(2)}\eta_2^2+A_2^{(2)}\eta_2^4+A_3^{(2)}\eta_2^6+g_1^{(2)}(\eta_{2,x}^2+\eta_{2,y}^2)+g_2^{(2)}\eta_{2,x}\eta_{2,y}+F_C(M_5,\Gamma_1,\Gamma_3)+F_L(\Gamma_1)+F_L(\Gamma_3)$

$F_{GL}(28;X_4)=A_1^{(3)}\eta_3^2+A_2^{(3)}\eta_3^4+A_3^{(3)}\eta_3^6+g_1^{(3)}(\eta_{3,x}^2+\eta_{3,y}^2)+g_2^{(3)}(\eta_{3,x}^2-\eta_{3,y}^2)F_C(X_4,\Gamma_1,\Gamma_2)+F_L(\Gamma_1)+F_L(\Gamma_2)$

$F_C(\Gamma_3,\Gamma_1)=C_1^{(1)}\eta_1^2\eta_4+C_2^{(1)}\eta_1^2\eta_4^2$, $F_C(M_5,\Gamma_1,\Gamma 3)=C_1^{(2)}\eta_2^2\eta_4+C_2^{(2)}\eta_2^2\eta_1+C_3^{(2)}\eta_2^2\eta_4^2+C_4^{(2)}\eta_2^2\eta_5^2+C_5^{(2)}\eta_2^2\eta_4\eta_5$,

$F_C(X_4,\Gamma_1,\Gamma_2)=C_1^{(3)}\eta_3^2\eta_4+C_2^{(3)}\eta_2^2\eta_4^2+C_3^{(3)}\eta_2^2\eta_5^2$

$F_L(\Gamma_1)=A_1^{(4)}\eta_4+A_2^{(4)}\eta_4^2+A_3^{(4)}\eta_4^3+A_4^{(4)}\eta_4^4$, $F_L(\Gamma_2)=A_1^{(5)}\eta_5^2+A_2^{(5)}\eta_5^4$, $F_L(\Gamma_3)=A_1^{(6)}\eta_1^2+A_2^{(6)}\eta_1^4$

$$\partial F(\xi)/\partial\eta=(\partial F/\partial\eta)(\partial\eta/\partial\xi). \quad (3)$$

A periodic dependence on atomic displacements results naturally from successive special values of the strain and/or displacements of the structure at which there is an additional onset of symmetry. The Ginzburg-Landau (GL) free energies and the lock-in values for each of our mechanisms are given in columns 4 and 5, respectively, of Table III.

In order to display the allowed transitions for various ranges of coefficients we construct an effective free energy in terms of just our primary OP. Since we keep only up to sixth degree terms, there is only one effective free energy expansion for the three mechanisms we obtained. The phase diagram for the single component primary OP's (all three of our mechanisms) is shown in Fig. 4, p. 150, of Ref. 1.

Conclusion. We have developed a systematic formalism that uses space group and site symmetries to the fullest extent in order to enumerate transition paths corresponding to single primary OP's. Coupled primary OP's could also be considered yielding additional mechanisms. However, two pieces of information in our theory depend on the microscopic interactions and must be obtained for a specific material either from experimental structural data (where available) or from electronic structure and molecular dynamics calculations. These are the specific transformation path and the specific functional dependence of the OP η on the distortion coordinate ξ for a given material. For the sake of simplicity/illustration one could choose a polynomial form whose roots are the special values of the distortion in the two phases. Nonetheless, other forms such as the transcendental order parameter[4] are also acceptable.

Our procedure is generally applicable to other reconstructive transitions such as bcc→fcc, hcp→ω, bcc→ω, hcp→ fcc, graphite→diamond, etc. A very interesting example is a possible diamond→bcc quantum crystal transition in carbon in the core of certain white dwarfs.[5] Our approach can also include order-disorder and other types of mechanisms (e.g., axial OP's) through the association of these properties with appropriate IR's. Finally, our specific results here are also applicable to many different physical systems since the square lattice to triangular lattice transition is observed in flux line lattices[6] and vortex lattices[7] in superconductors, Wigner crystals in 2D electron gas,[8] skyrmion crystals in quantum Hall systems,[9] etc.

We acknowledge insightful discussions with E. Mottola, W. Klein, and R.C. Albers. This work was supported by the U.S. Department of Energy.

[1] P. Tolèdano and V. Dmitriev, *Reconstructive Phase Transitions* (World Scientific, Singapore, 1996).

[2] D. M. Hatch *et al.*, Phys. Rev. B **35**, 4935 (1987); H. T. Stokes *et al.*, *ibid.* **43**, 11 010 (1991).

[3] H. T. Stokes and D. M. Hatch, *Isotropy Subgroups of the 230 Crystallographic Space Groups* (World Scientific, Singapore, 1988). The software package ISOTROPY is available at http://www.physics.byu.edu/~stokesh/isotropy.html

[4] V. P. Dmitriev *et al.*, Phys. Rev. Lett. **60**, 1958 (1988).

[5] D. E. Winget *et al.*, Astrophys. J. Lett. **487**, L191 (1997); G. Chabrier *et al.*, Nature (London) **360**, 48 (1992).

[6] M. R. Eskildsen *et al.*, Phys. Rev. Lett. **78**, 1968 (1997).

[7] B. Keimer *et al.*, J. Appl. Phys. **76**, 6778 (1994); Phys. Rev. Lett. **73**, 3459 (1994); D. Chang *et al.*, *ibid.* **80**, 145 (1998).

[8] J. Medeirosesilva and B. J. Mokross, Phys. Rev. B **21**, 2972 (1980); A. Holz, *ibid.* **22**, 3692 (1980); L. Glasser and A. G. Every, J. Phys. A **25**, 2473 (1992).

[9] V. Bayot *et al.*, Phys. Rev. Lett. **76**, 4584 (1996); M. Rao *et al.*, *ibid.* **79**, 3998 (1997).